ELSEVIER

Journal of Nuclear Materials 245 (1997) 34–43

journal of nuclear materials

Liquid metal embrittlement of Zr–2.5% Nb alloy

B. Cox *, Y.-M. Wong

Centre for Nuclear Engineering, University of Toronto, 184 College Street, Toronto, Ont., Canada M5S 3E4

Received 25 September 1996; accepted 10 December 1996

Abstract

Liquid metal embrittlement (LME) of zirconium alloys in mercury is entirely transgranular. Grains not oriented for pseudo-cleavage on the basal plane fail by slip on the prism planes to form the characteristic 'fluting'. Because of this, fracture in Hg of Zr–2.5 Nb small compact tension specimens (cut from five different CANDU pressure tubes) showed large differences in the macroscopic fracture topography that could be related to differences in the local continuity of the basal planes in the structure, even though the average textures were very similar. These differences could be related to differences in the fracture toughness of the tubes. Although LME in zirconium alloys has been thought to be generally transgranular because of previous experience in Hg, Cs/Cd mixtures, a Hg/In/Tl eutectic, and Li, tests in Ga showed no transgranular cracking, but small amounts of intergranular cracking were observed that appeared to be limited by poor wetting of Zr by Ga.

1. Introduction

In many ways the term liquid metal embrittlement (LME) is a misnomer, since it has long been known that solid metals near to their melting points can cause embrittlement [1,2] and that metal vapor embrittlement (MVE) is possible if the embrittling metal has an adequate vapor pressure at the temperature of cracking [3]. However, LME is the colloquial term that is generally used to cover all cases. Early studies of LME in cubic metals [4,5] showed that it was usually intergranular (IG), and it became expected that all LME would be IG. This situation changed when it was observed that LME of Zircaloy-2 in mercury at room temperature consisted entirely of transgranular (TG) pseudo-cleavage on (or near to) the basal plane, coupled with 'fluting' caused by ductile slip on the prism planes [6–9]. The idea that LME or MVE in zirconium alloys should always be TG was further encouraged by the observation that cracking in Cs and Cs/Cd vapors showed no intergranular features, and often no 'fluting' if the texture was such as to provide a continuous path along the basal planes [3]. However, it was reported elsewhere [10] that embrittlement by cadmium was intergranular, and in our tests [3,11] the crack initiation was intergranular, with TG propagation (Fig. 1a). This seemed to be a unique example, as Cd additions to Cs did not result in any IG features.

Interest in LME of zirconium alloys has lapsed since it became evident that pellet-clad interaction failures in nuclear fuel cladding were almost certainly caused by iodine fission products and not by caesium [3,12,13]. Recently, however, the uniquely TG cracking of zirconium alloys in Hg became attractive for examining local texture variations through the wall in Zr–2.5% Nb pressure tubes having similar average textures [14]. More recently proposals to use gallium to provide good heat transfer between UO_2 and the Zircaloy cladding in some experimental fuel elements have caused us to look at the possible extent of LME of zirconium alloys in liquid Ga. Gallium is an aggressive cracking agent for Al, Cd, Fe, Ag, Sn and Zn, but was not known to crack Ti or Zr [5]. The development of brazes for zirconium alloys would also need to address

* Corresponding author. Tel.: +1-416 978 2127; fax: +1-416 978 4155.

PII S0022-3115(96)00752-0

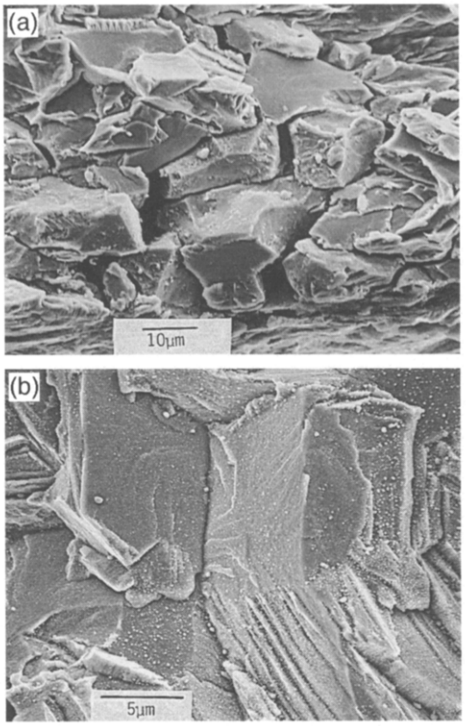

Fig. 1. Liquid metal embrittlement of Zircaloy-2. (a) IG crack initiation and TG crack propagation in Cd, (b) Completely TG cracking by Ag resulting from spot welding [11].

the question of LME susceptibility if Ag was a component (Fig. 1b) [11].

2. Experimental

Tests were carried out using small compact tension (CT) specimens cut from Zr–2.5% Nb alloy pressure tubes of CANDU design. Samples from five tubes showing different fracture toughnesses when tested in air [14–16] were modified to provide a crack starter V rather than a straight notch (Fig. 2). K_{LME} values for Zr alloys in Hg are low, and these specimens are not long enough for the crack to arrest before reaching the end of the specimen. Crack velocities are also too high to measure easily in such

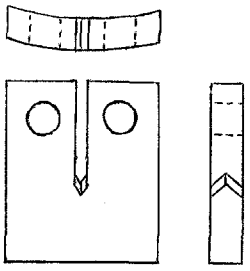

Fig. 2. Diagram of compact tension specimen modified for LME testing (approx. twice full scale).

a short specimen. Thus these samples were expected primarily to give qualitative differences in the fracture morphology for the different tubes tested. The tubes and their fracture toughness values are listed in Table 1. Previous work had shown the importance of ensuring the wetting of a freshly produced zirconium surface by the liquid metal when starting an LME crack [6–8]. Most liquid metals do not wet the ZrO_2 film that is always present on a Zr alloy surface at low temperatures. Wetting of the freshly produced fracture surface can be judged after breaking the specimen by the presence of a 'metallic mirror' of the liquid metal on the fracture. To maximize the probability of getting wetting at the start of crack formation the geometry should be such as to keep the liquid metal in contact with the point where the first fresh surface is expected to form. Thus, the notch regions of the modified CT specimens were converted into small cells to contain the liquid metal by using transparent sticky-tape on both sides of the slot. This provides a deformable cell that will contain the liquid metal throughout the test and thus keep the liquid metal in contact with the tip of the starter V. Specimens modified in this way were pulled on a Hounsfield tensiometer because the horizontal pull of this machine allowed the liquid metal in the cell to maintain its contact with the starter V, and hence gave the best chance of obtaining good wetting as quickly as possible of the first fresh Zr surface produced. Early studies had shown that prefatigued samples repassivated too quickly for good wetting to be obtained [6]. The liquid metal cells so produced were filled using a hypodermic syringe and were checked to make sure that the liquid metal went right to the bottom of the cell by shining a flashlight through the

Table 1
Zr–2.5 wt% Nb alloy tubes cracked in Hg and Ga

Tube No.	β-quench	Fracture	Toughness [14] dJ/da (MPa)	LME	Description of fracture
H190M	yes	high	243	Hg	highly serrated, TG + fluting
1037	no	high	216	Hg	highly serrated, TG + fluting
H850	no	high	353	Hg	highly serrated, TG + fluting
H737	no	medium	161	Hg	small serrations, short length, TG + F
622	no	low	153	Hg	flat fracture, TG + fluting, striations
622	no	low	153	Ga	short planar crack, 0.3 mm max., IG.

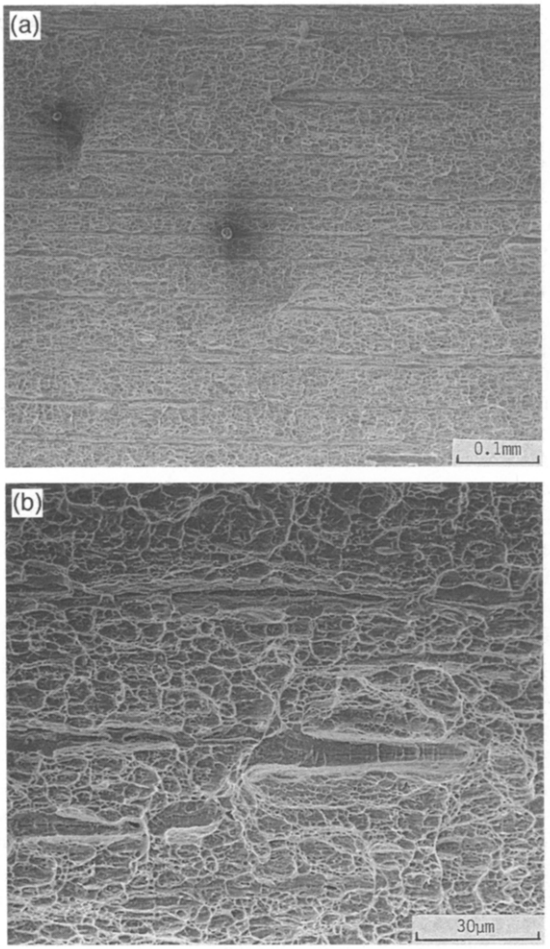

Fig. 3. Ductile fracture of specimen 622-F9.

transparent tape from the back side of the cell. Tests in mercury were conducted at room temperature, and a small amount of In and Tl were added to the mercury to improve the wetting of the Zr [6]. Hg/In/Tl mixtures wet ZrO_2 reasonably well when fresh, thus a 'metallic mirror' can be produced on ZrO_2 by these mixtures. Wetting the surface ZrO_2 film with the liquid metal improves the chances of quickly wetting the first fresh Zr fracture surface to be produced. Those specimens cracked in gallium were maintained above the melting point of gallium (30°C) by use of a hair dryer, but no wetting additives were added, as it would not have been possible to establish whether Ga had been the active species in producing any subsequently observed brittle fractures.

Specimens were pulled at a constant rate of crack opening displacement (COD) of about 0.05 mm s^{-1} for both Hg and Ga tests. It appeared that wetting of the fresh Zr surface was a problem in tests in Ga (six nines purity) so one test was carried out where the COD was increased in 0.1 mm steps with a pause of 2–3 s between each step, and a longer pause of ~ 10 s every 0.5 mm This stepwise extension made no difference to the extent of LME fracture observed on the broken faces of the specimens. No evidence was found of any 'metallic mirrors' on the fracture surfaces produced in gallium. The fractured faces were examined using a scanning electron microscope, and stereo-pairs were used to assess the serrated nature of some fractures.

3. Results

The fractography of a CT specimen of tube 622 broken in air is shown in Fig. 3. The fracture was largely ductile,

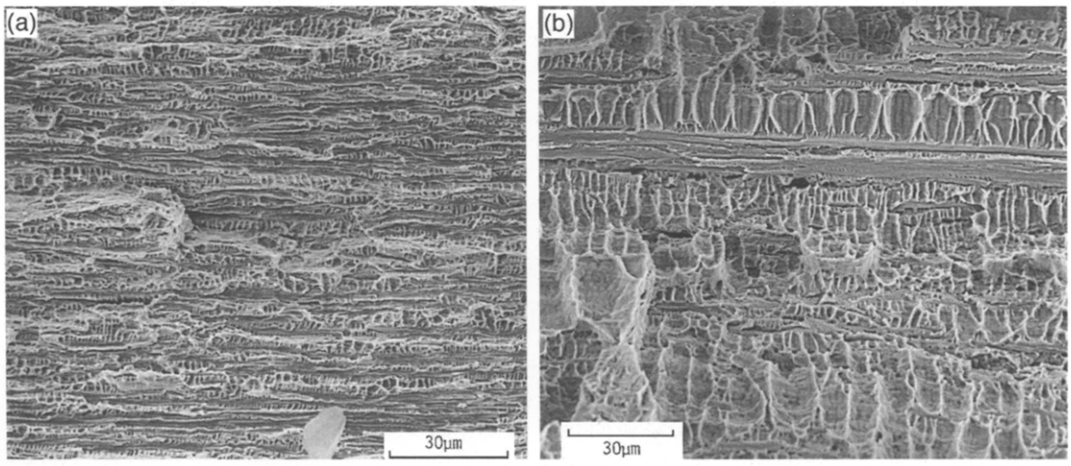

Fig. 4. TG pseudo-cleavage and ductile fluting (a) in a relatively planar fracture of tube 622 in Hg, and (b) in the vertical wall of a large serration in tube H850. Note the features are the same but the scale is different because the width of the α-Zr grains is much less in the radial–longitudinal plane (a) than it is in the circumferential–longitudinal plane (b).

but long striations or fissures were found running in the longitudinal direction of the original tube (and of the CT specimen). These non-ductile features were the subject of the study of fracture toughness variability that gave rise to this project [14–16].

Fractures in Hg showed the expected transgranular features separated by ductile fluting (Fig. 4). Since the basal poles in CANDU pressure tubes are predominantly circumferential this means that the planes on which easy LME fracture occurs were usually normal to the average plane of crack propagation. Variations in the continuity of these basal planes in the structure led to big variations in the extent of serrations seen in the fractures (Figs. 5–7). In the most serrated fractures the webs between the fractured basal planes failed in shear (Figs. 8 and 9) rather than by fluting. In other cases the fractures were less serrated and TG cracking and fluting were seen throughout the relatively planar fractures (Fig. 4a). The non-ductile striations seen in fractures in air in tube 622 could also be seen in the LME fractures of the same tube, where they appeared like any other TG facet, showing that these features failed under similar conditions to the TG pseudo-cleavage on the basal planes that allowed the propagation of LME cracks. More details of the fractography in Hg are given in Refs. [17,18].

Fractures in Ga showed no evidence, in the form of remaining 'metallic mirrors' on any part of the fresh surface, for the wetting of the fracture surface by the liquid

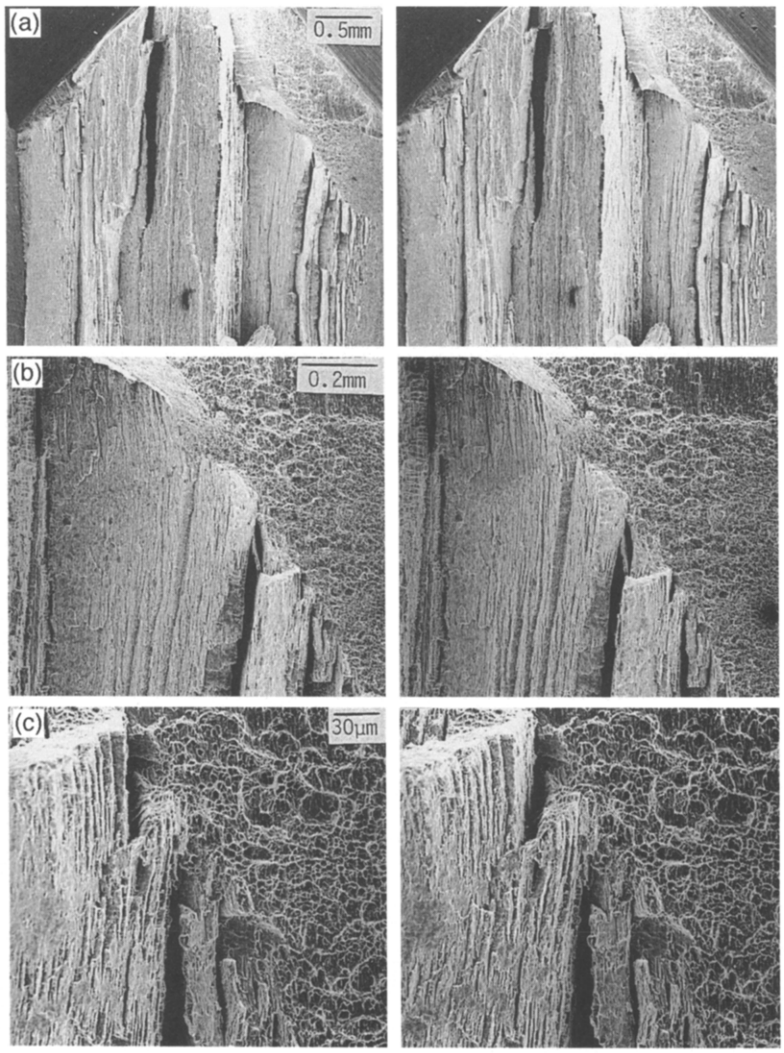

Fig. 5. Stereopairs of specimen H850-E9 cracked in Hg. (a–c) are of the very serrated fracture at the start of the crack; (b) is an enlarged view of the right center of (a); (c) shows more detail of the bottom right of (b). The change from ductile to LME fracture is visible at the top R of each pair. The fracture remained serrated along the whole length of the crack. Serrations have one vertical wall showing LME fracture (Fig. 3b) while the other is mainly shear. Cracks propagate from top to bottom of pictures.

Ga. The fractures were largely ductile, however, a small region of non-ductile fracture could always be found at the crack starting point (Figs. 10 and 11). This brittle fracture had a maximum extent of 0.2–0.3 mm and was not transgranular. By analogy with earlier stress corrosion cracking tests on Zr–2.5% Nb pressure tubes in fused salt media containing chlorides [19,20], which were intergranular (Fig. 12), it appeared that this cracking in Ga was also intergranular.

4. Discussion

The cracks in mercury started as a ductile crack near the tip of the starter V and in some instance propagated for some distance before wetting induced a change over to a brittle LME fracture. In other instances only traces of ductile failure were found at the start of the crack and an almost immediate change to LME was observed. The fractures of the high fracture toughness tubes were all highly serrated (Figs. 5 and 13) whereas the low fracture toughness tube showed a relatively planar fracture on a macroscopic scale (Fig. 4a). In some instances there were numerous aborted attempts to develop cracks parallel to the principal stress in the specimen before the large serrations were able to develop (Fig. 13). The fractography of the brittle crack propagation faces was a similar mixture of transgranular pseudo-cleavage and ductile fluting (Fig. 4) whether the plane of the LME crack was normal to the principal stress (i.e., cracks in the radial/longitudinal plane

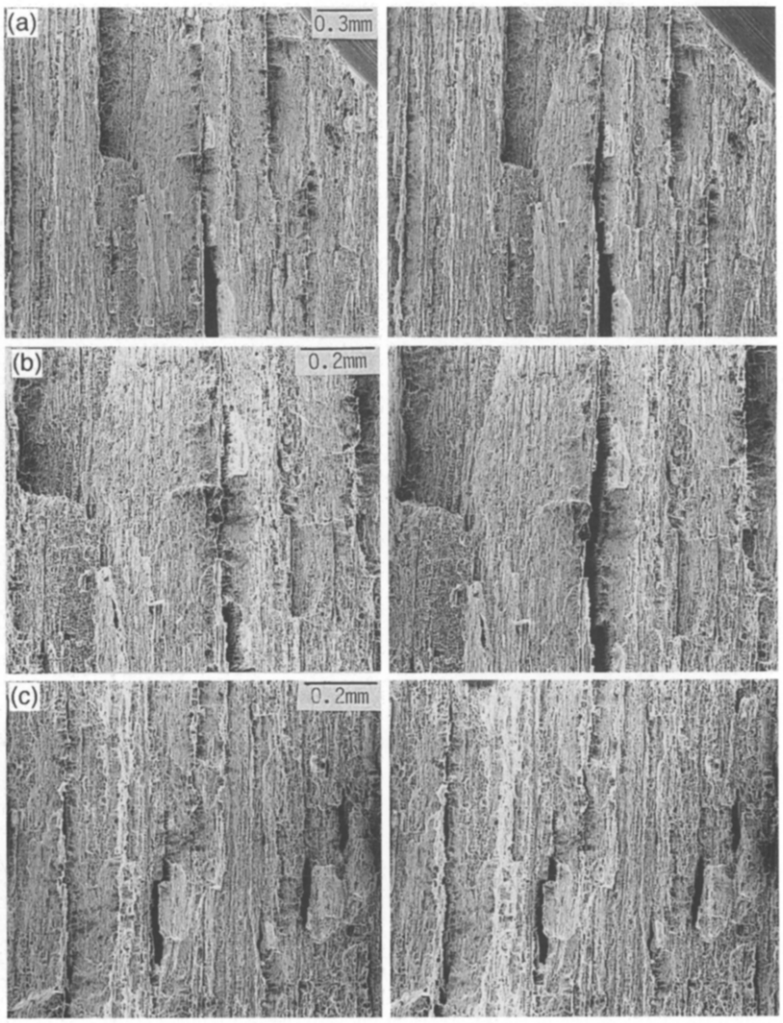

Fig. 6. Stereopairs of specimen H737-D9 cracked in Hg. The specimen showed very little ductile fracture at the start of the crack (a). The crack face was heavily serrated with the shear fracture primarily visible (b); the serrations diminished somewhat in severity as the crack propagated (c). Cracks propagate from top to bottom of pictures.

of the tube) or parallel to it (i.e., cracks in the circumferential/longitudinal plane of the tube). This suggests that the low fracture toughness tube had sufficient grains with basal poles in or near the circumferential direction to allow the crack to propagate primarily in the radial/longitudinal plane over the whole specimen cross-section. By contrast, the high fracture toughness tubes appear to have had regions of high basal plane continuity in the circumferential/longitudinal plane, especially in the center of the tube wall.

This result was something of a surprise because the texture of CANDU pressure tubes is designed to have the greatest density of basal poles in the circumferential direction. All the high fracture toughness tubes did show significant areas of flat fracture in the radial/longitudinal plane near both of the tube surfaces (Fig. 12) and the very large serrations in the fractures were usually in the center of the tube wall. This could result from a change in the stress state to near plane stress conditions near the tube surface, which reportedly affects the number of fissures observed in fracture toughness tests [16]. However, LME requires the presence of suitably oriented basal planes, which are not necessary for a ductile fracture mode, and occurs under both plane stress and plane strain conditions [6]. Thus it is possible that all the tubes could have had very similar average textures (or that the texture measurements preferentially obtained the X-ray signal from near the tube surface), with only the high fracture toughness tubes having one or more layers near the center of the wall where there was a high continuity of basal planes in the circum-

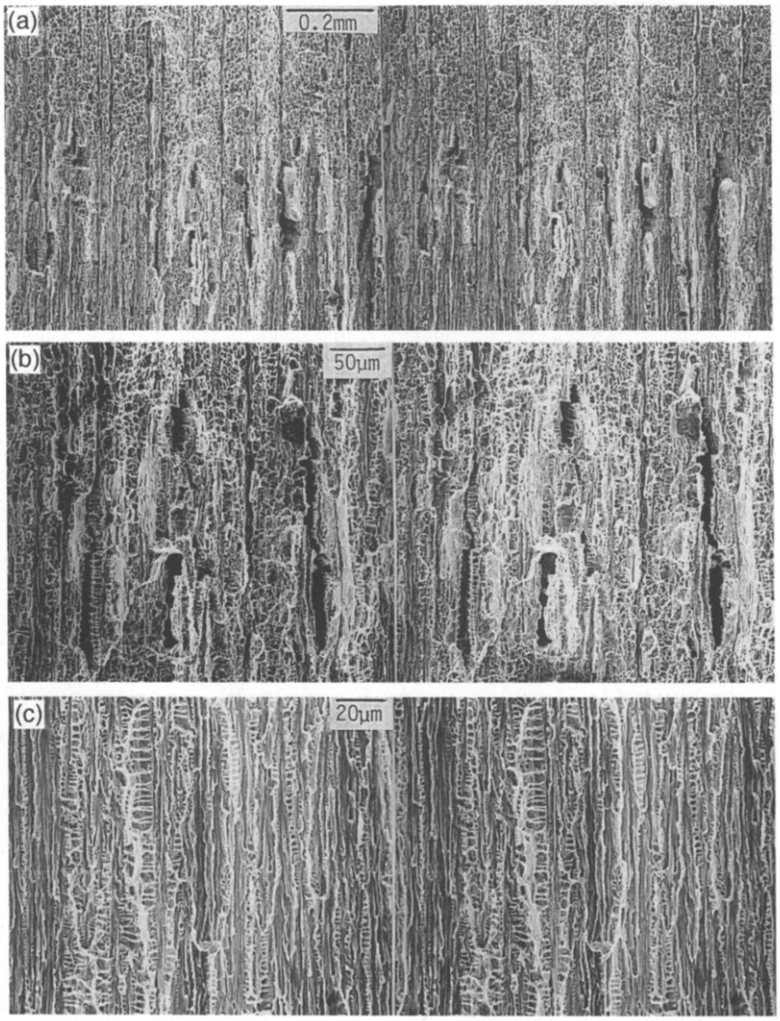

Fig. 7. Fracture surface of low fracture toughness tube specimen 622-F9 in Hg. (a) Transition from ductile to brittle LME fracture. Note that a few attempts to generate serrations all fail. (b) Enlarged view of this transition region in the center of (a). (c) Fully developed relatively planar fracture further along crack. Cracks propagate from top to bottom.

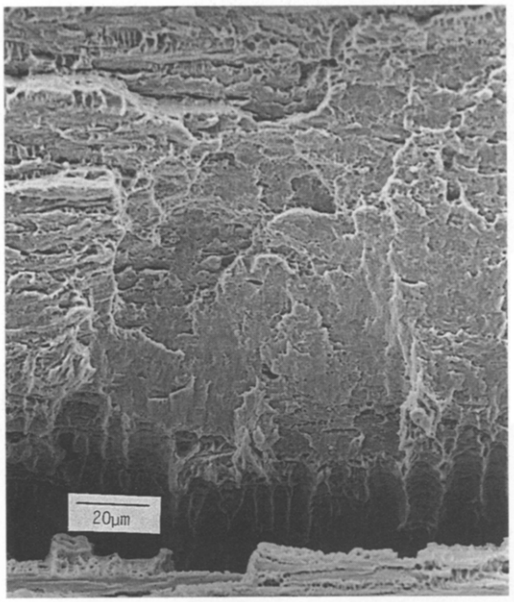

Fig. 8. Shear failure of the sloping wall of a large serration in the fracture surface of specimen H850-E9.

ferential/longitudinal plane [14]. Recent texture measurements by neutron diffraction and acoustic velocity analysis [21] have confirmed that the average spread of basal poles into the circumferential/longitudinal plane is greater than would be expected from the X-ray texture measurements, and from the observed variations in acoustic velocity and microhardness across the wall thickness it is possible that these grains are localized in bands to give the serrated fractures observed in the high fracture toughness tubes. However, there is insufficient evidence of local variations in tube texture through the tube wall available from these other sources to permit a correlation with the LME results. Such layers would contribute correspondingly aligned regions of prismatic slip during a fracture toughness test which might explain the high toughness of these tubes since enhanced ductility would be associated with such layers. An explanation has been preferred for the low fracture toughness of some tubes based on the presence of the low ductility striations seen in their fracture surfaces. These appear to have resulted from high carbon, chlorine and phosphorus impurity levels in these regions [14,15,22]. Reduction of these impurity concentrations, especially chlorine, by a fourth arc-melting step appears to have eliminated such striations (and low fracture toughness tubes) [23].

The cracking observed in gallium was very limited, and appeared to be so limited because of very poor wetting. When pulled at a constant strain rate of 0.05 mm s^{-1} the fracture was almost entirely ductile, but a small area of intergranular fracture (Fig. 10) was observed at the crack start, and extended a maximum of 0.3 mm. This brittle IG crack never developed into a large area of IG fracture. When the stress was increased in small increments rather than continuously a small region of intergranular cracking still formed at the crack starter, and also changed to a ductile failure after a maximum of ~ 0.3 mm of intergranular cracking (Fig. 11). The features of these IG cracks are very similar to those observed for cracking in fused salts

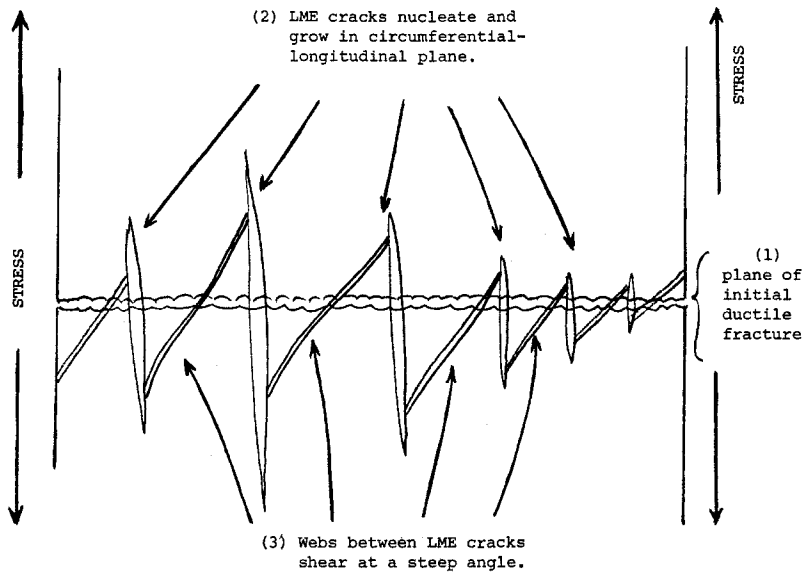

Fig. 9. Proposed sequence of steps in the production of the highly serrated fracture surfaces in tubes H737 and H850.

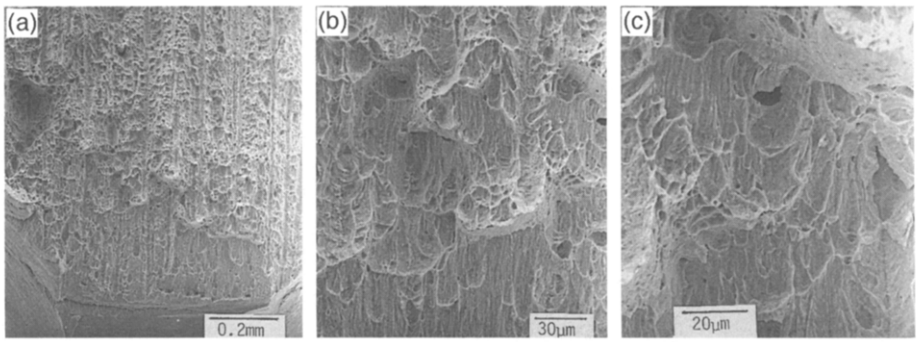

Fig. 10. Fracture of specimen 622-05 in liquid gallium at a constant strain rate of 0.05 mm s^{-1}. Note the 'thumb nail' of intergranular fracture at the crack starting point in (a), changing to completely ductile fracture (with striations of low energy fracture) at top. (b) Boundary between 100% IG fracture at bottom and a region where some uncracked webs fail in a ductile manner. (c) boundary between still partially IG fracture and completely ductile failure. A low-energy failure striation in the ductile fracture region of (a) can be seen to have initiated at right of center in (b) without any evidence of a cracked particle being present. The α-Zr grains in Zr–Nb pressure tubes are very elongated in the longitudinal direction (the vertical direction in each picture). The crack propagated from bottom to top.

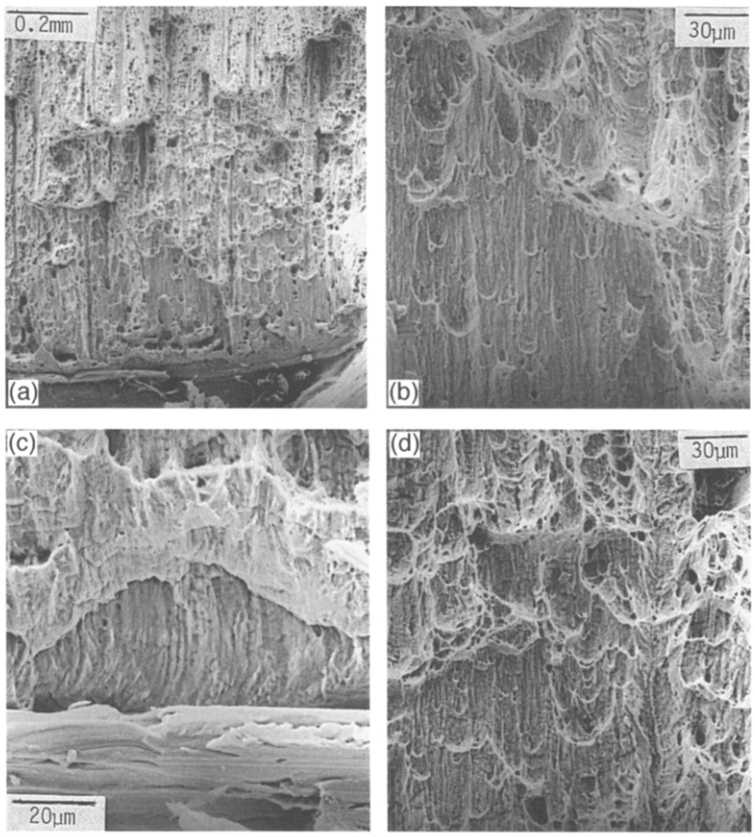

Fig. 11. Fracture of specimen 622-09 in liquid gallium when strain was increased in increments of 0.1 mm (40 steps to failure). Note the more irregular IG crack initiation area broken by several low-energy fracture striations that continue into the ductile fracture (a). IG fracture at left of (b) with a striation on the right. Again no evidence of a cracked particle at the start of the SLEF. (c) 100% IG crack initiation site with the metal grains bent by the machining of the notch. (d) Boundary between IG fracture and ductile failure with a SLEF passing from one to the other at right. Crack propagates from bottom to top.

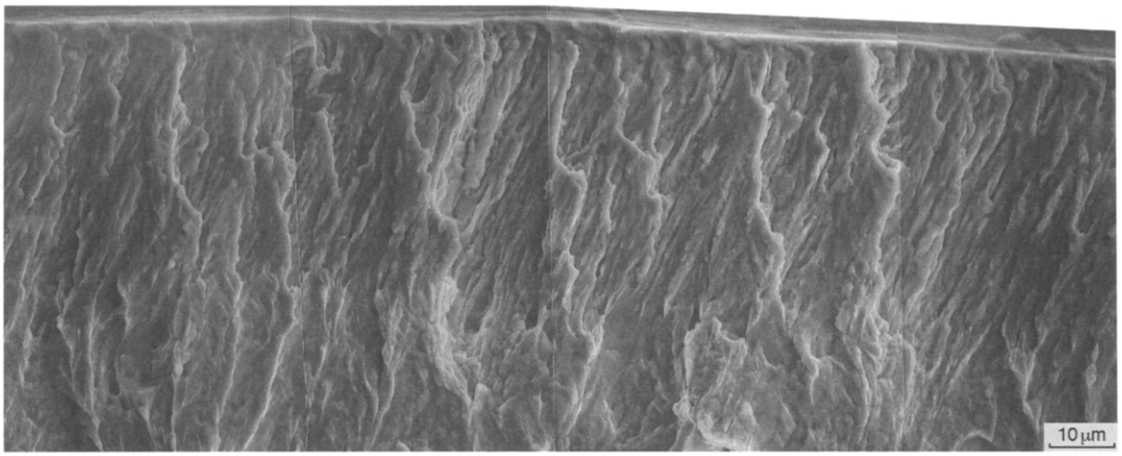

Fig. 12. IG crack initiation at the edge of a round notched bar cut from a Zr–Nb alloy pressure tube and cracked in a molten salt containing chloride [19]. Again note the bending of the elongated α-Zr grains by the machining of the notch.

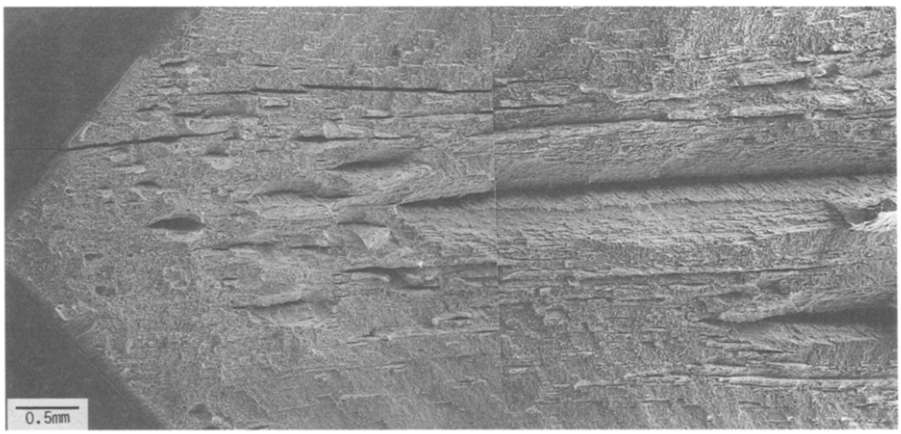

Fig. 13. Fracture surface of specimen H190M-C9 in Hg showing a number of aborted attempts to develop cracks in the circumferential–longitudinal plane before the large serrations become established. Note the relatively planar crack morphology near the specimen surfaces, and that one of the first cracks in the plane normal to the main fracture has run back into the unstressed notch.

Table 2
Metals known to cause at least some embrittlement of Zr

Embrittling element	Zr alloy	Type of test [a]	Refs.
Li [b]	Zircaloy-2	ZrB alloy irrad. + UT	[24]
Cs	Zircaloy-2	SIMFEX, bend UT, DCB	[3,6,9,10,25]
Cd	Zircaloy-2	SIMFEX, UT	[10,11,25]
Cs/Cd	Zircaloy-2	SIMFEX, UT, C Tube	[10,25]
Cs/Ca	Zircaloy-2	UT	[10]
Cs/Sr	Zircaloy-2	UT	[10]
Cs/Y	Zircaloy-2	UT	[10]
Cs/Zn	Zircaloy-2	UT	[10]
Ag	Zircaloy-2	Ag spot-welded to Zr, bend	[11]
Hg	Zirc-2, Zr-2.5 Nb	DCB, CT, bend	[6–9], this work
Ga	Zr–2.5 Nb	CT	this work

[a] UT – uniaxial tensile test; DCB – double cantilever beam; CT – small compact tension; SIMFEX – simulated fuel expansion test; C tube – compressed tube test.

[b] This test was designed to show the effect of He bubbles produced under irradiation on tensile properties at 300°C. A Zircaloy-2/boron alloy was prepared and irradiated; annealed at 800°C to grow He bubbles; and tested under uniaxial conditions. The fracture surface was brittle, contained few He bubbles, and was almost 100% TG pseudo-cleavage.

containing chlorides (Fig. 12), where the grain structure at the surface showed the same deflection as a result of machining [20]. It is possible that a minor impurity addition to the gallium could improve its wetting of zirconium and result in more extensive cracking. Such synergistic effects of minor impurities have been commonly observed in LME [4,5]. If the use of Ga inside an instrumented fuel pin were still contemplated then fission products such as Cs, Cd or In should be investigated as possibly impurities that could improve the wetting of Zr. The 'tailing' of Hg as a result of traces of I_2 is well known, and the possibility of some synergistic effects of I_2 fission products and Ga would also need to be investigated. No attempt has been made here to look for minor additives to the gallium that might improve its wetting of zirconium surfaces, and hence the severity of the cracking.

The metals that are currently known to produce at least some cracking of zirconium alloys are listed in Table 2. The number is now becoming quite large, and it is tempting to surmise that some other metals (e.g., Na, K) which showed no evidence for cracking in uniaxial tensile tests [10], might cause cracking in a fracture toughness type test, because of evidence for cracking by other alkali metals (Li, Cs).

5. Conclusions

Differences in the fracture morphology in Hg of different Zr–2.5% Nb pressure tubes has been demonstrated to correlate with the fracture toughnesses of the tubes measured in standard j-integral tests. These differences in LME fracture must relate to differences in basal plane continuity through the tube walls, since cracking in mercury occurs only on basal planes. Insufficient details of the local texture variations in these tubes are available for a detailed comparison of texture differences.

Small amounts of intergranular LME in gallium have been observed, and may be limited by the wettability of Zr by Ga. Tests to establish whether common fission products might improve wettability should be done before using Ga in contact with Zr fuel cladding.

Acknowledgements

The authors are grateful to Atomic Energy of Canada Ltd., through the CANDU Owner's Group, and the Natural Sciences and Engineering Research Council of Canada for the funding that has allowed this research to proceed, and to Dr Pauline Davies (AECL) for supplying the specimens and commenting on the results. The help of Bernie Surette (CRL) in searching his files for the negatives of the micrographs in Fig. 1 is greatly appreciated.

References

[1] D.N. Fager and W.F. Spurr, Corrosion 26 (1970) 409.
[2] D.A. Meyn, Corrosion 29 (1973) 192.
[3] B. Cox, B.A. Surette and J.C. Wood, 'Pellet-clad interaction failures: Stress corrosion cracking by iodine or metal vapour embrittlement by cesium/cadmium vapours?', Proc. 2nd Int. Conf. on Environmental Degradation of Engineering Materials, Vol. 2 (1981) p. 293.
[4] W. Rostoker, J.M. McCaughey and H. Markus, Embrittlement by Liquid Metals (Reinhold, New York, 1960).
[5] M.H. Kamdar, Prog. Mater. Sci. 15 (1973) 289.
[6] B. Cox, Environmentally induced cracking of zirconium alloys II. Liquid metal embrittlement, Atomic Energy of Canada Ltd., Chalk River, Report AECL-3612 (1970).
[7] I. Aitchison and B. Cox, Corrosion 28 (1972) 83.
[8] B. Cox, Corrosion 28 (1972) 207.
[9] B. Cox, 'Identifying the failure mechanisms of zirconium alloys from fractographic studies', Proc. Symp. on Metallography and Corrosion (NACE, Houston, TX, 1986) p. 153.
[10] W.T. Grubb and M.H. Morgan III, 'A survey of the chemical environments for activity in the embrittlement of Zircaloy-2', Proc. 4th Int. Conf. on Zirconium in the Nuclear Industry, ASTM-STP-61 (1979) p. 145.
[11] B.A. Surette and D.A. Adkins, Atomic Energy of Canada Ltd., Chalk River (1977), unpublished results.
[12] B. Cox, J. Nucl. Mater. 170 (1990) 1.
[13] B. Cox, J. Nucl. Mater. 172 (1990) 249.
[14] I. Aitchison and P.H. Davies, J. Nucl. Mater. 203 (1993) 206.
[15] P.H. Davies and R.S.W. Shewfelt, in: Proc. 11th Int. Symp. on Zirconium in the Nuclear Industry, eds. G.P. Sabol and R.E. Bradley, ASTM-STP-1295 (1996) p. 492.
[16] P.H. Davies, R.R. Hosbons, M. Griffiths and C.K. Chow, in: Proc. 10th Int. Symp. on Zirconium in the Nuclear Industry, eds. A.M. Garde and E.R. Bradley, ASTM-STP-1245 (1995) p. 135.
[17] B. Cox, Textural Inhomogeneities in Zr–Nb Pressure Tubes, Center for Nuclear Engineering, Report CNEUT-91-05 (1991).
[18] B. Cox and Y-M. Wong, Effect of β-quenching on LME of Zirconium–2.5% Niobium alloy pressure tubes, Center for Nuclear Engineering, Report CNEUT-91-07 (1991).
[19] B. Cox, Oxid. Met. 3 (1971) 399.
[20] B. Cox and S.A. Aldridge, J. Nucl. Mater. 67 (1977) 55.
[21] J.F. Bussiere, A. Moreau et al., Proc. of ASME Pressure Vessel Conf., Montreal, July (1996).
[22] P.H. Davies, I. Aitchison, D.D. Himbeault, A.K. Jarvine and J.F. Watters, Fatigue Fract. Eng. Mater. Struct. J. 18 (1995) 789.
[23] J.R. Theaker, R. Choubey, G.D. Moan, S.A. Aldridge, L. Davis, R.A. Graham and C.E. Coleman, in: Proc. 10th Int. Symp. on Zirconium in the Nuclear Industry, eds. A.M. Garde and E.R. Bradley, ASTM-STP-1245 (1995) p. 221.
[24] C.E. Ells and I. Aitchison, Atomic Energy of Canada Ltd., Chalk River, private communication.
[25] J.C. Wood, B.A. Surette, I.M. London and J. Baird, J. Nucl. Mater. 57 (1975) 155.